Preferred citation: R. Eckhart, M. Donoser and W. Bauer. Single fibre flexibility measurement in a flow cell based device. In **Advances in Pulp and Paper Research, Oxford 2009**, *Trans. of the XIVth Fund. Res. Symp. Oxford, 2009*, (S.J. I'Anson, ed.), pp 247–271, FRC, Manchester, 2018. DOI: 10.15376/frc.2009.1.247.

SINGLE FIBRE FLEXIBILITY MEASUREMENT IN A FLOW CELL BASED DEVICE

Rene Eckhart[1], *Michael Donoser*[2] *and Wolfgang Bauer*[1]

[1] Institut for Paper, Pulp and Fibre Technology
[2] Institute for Computer Graphics and Vision, Graz University of Technology

ABSTRACT

Single fibre flexibility is widely recognised as an important parameter in the papermaking process. A novel flow cell based method for its measurement was developed at the Institute for Paper, Pulp and Fibre Technology at Graz University of Technology. A special flow channel geometry is used to induce high shear forces in a laminar flow regime. The movement of single fibres passing the highly sheared region is recorded by means of a high speed image acquisition system. Based on the reactions of the fibres to the fluid forces a flexibility parameter is determined for each evaluated fibre.

1 INTRODUCTION

Fibre flexibility is a parameter of fundamental importance in the sheet consolidation process and in fibre to fibre bonding. It affects paper properties in a way that fibres with higher flexibility form a denser sheet with more fibre to fibre bonds of increased area. Paper properties like apparent sheet density and porosity, paper strength properties, surface smoothness and optical properties are affected. Therefore the measurement of fibre flexibility is of considerable importance for pulp characterization based on fibre morphological parameters.

Today pulp characterization is increasingly performed on a single fibre basis by flow cell analysis where a highly diluted fibre suspension is pumped through a transparent cell and images of individual fibres are captured for image analytical evaluation. These commercially available flow cells show good on line applicability and deliver distributions of morphological parameters like fibre length, width, curl and kink. Some of these flow cells already offer an average flexibility index that is based on the average fibre curl at different shear rates [1] (e.g. *FibreMaster*™, MorFi fibre analyser) but cannot deliver single fibre values or distributions.

Several fibre flexibility measurement methods are mentioned in the literature, some of them single fibre based, some evaluating the fibre network. Kuhn *et al.* [2] grouped the existing fibre flexibility measurement methods depending on their measurement principle: bending beam methods, classification methods, conformability methods and network methods. As the new method presented in this paper is based on the movement of single fibres in sheared suspension and thus on the deformation due to hydrodynamic forces, only methods with a related measurement principle shall be discussed at this point.

Samuelson [3] developed a method where fibres are fixed in a clamp to the wall of a channel and exposed to a laminar water flow. The bending of the fibre due to the hydrodynamic load is observed through a microscope. Flow rate and corresponding fibre deflection are used to calculate fibre flexibility. Tam Doo and Kerekes [4] deflected the fibre as a simply supported beam. The fibre is placed across the notched tip of a glass capillary tube. A hydrodynamic drag force caused by a water flow around the fibre through the capillary tube is used to bend the fibre. The deflection is measured by visual observation through a microscope. This method is well known and was used by several authors dealing with the flexibility of pulp fibres. Both methods depend on a hydrodynamic load on the fibre but are rather time consuming as manipulation of single fibres is necessary. A bending beam method that does not depend on single fibre manipulation was presented by Kuhn *et al.* [5]. A capillary tube is entering a main channel and suspended fibres are transported through the capillary into the main channel flow. As a fibre exits the capillary it is deflected and deformed. The position and the form of the fibre were recorded using a CCD camera. The flexibility was then calculated using simple beam theory as the fibre was assumed to be momentarily at rest and in contact with the upstream and downstream sides of the capillary (pseudo steady state at the T-junction). All these methods apply bending beam theory to relate the deflection of the fibre under a known load to its flexibility and are therefore capable of delivering the flexibility in terms of the Young's modulus. The mechanical expression for the flexibility F [$1/Nm^2$] of a bending beam is defined as:

$$F = \frac{1}{EI} \tag{1}$$

$E[N/m^2]$ is Young's modulus in axial direction calculated from the mechanical behavior of the fibre under axial tension. $I[m^4]$ is the moment of inertia of the fibre's cross section.

Kuhn *et al.* [2] advanced their method by using a larger diameter capillary. That way the fibre exits the tube into the main channel without touching the wall and is deformed only due to the load of the fluid flow of the main channel. A CCD camera is used to collect two images of a specific fibre, one at the exit of the capillary (deformed state) and one downstream of the capillary (undeformed state). The fibre in these images is compared to fibres simulated under the same flow conditions. By matching the real fibre to this set of model fibres the fibre's flexibility is determined.

The first method considered a classification method according to Kuhn *et al.* [2] was also the first to take a look at the fibre motion in a sheared suspension. Forgacs *et al.* [6] looked at the rotational and translational movement of wood-pulp fibres suspended in a liquid subjected to laminar shear. The apparatus used for the experimental work is based on two concentric cylinders. These are rotated in opposite directions. Between them a so called Couette flow shows high shear forces under laminar conditions. A highly diluted fibre suspension is placed in the annulus between the cylinders. Individual fibres are selected in the stationary layer between the cylinders to be viewed with a microscope. The type of rotations and spins executed by a specific fibre depend upon whether the fibre is rather rigid or rather flexible. Based on these findings Meindersma *et al.* [7] developed a method to determine fibre flexibility. Due to sedimentation phenomenons and the needed high shear forces the liquid had to be of higher viscosity than water. They used different liquids in the apparatus to show suitable deformation of the fibres in laminar flow conditions.

The latter three of these are all based on fibres suspended in a liquid, the fibres are deformed due to hydrodynamic forces in a laminar flow field and the deformations are observed and related to the shear forces acting on the fibre. The same principles are used in our novel method which is introduced in this paper.

The aim was to develop a flow cell based method with on line applicability that determines single fibre flexibility and is capable to evaluate pulp samples statistically significant within reasonable time.

We have chosen an approach based on a flow cell that induces shear forces strong enough to deform pulp fibres suspended in water (in contrast to the methods demanding for a liquid with higher viscosity [6], [7]) and with a more simple flow geometry than the method already mentioned by Kuhn *et al.* [2]. The flow regime is laminar to ensure defined flow conditions that can be simulated and linked with the fibre's reactions to the fluid forces. A high speed image acquisition system is used to record the fibre's movement while passing the highly sheared region in the flow geometry. Automated image analysis and evaluation is used to determine a fibre's flexibility based on a sequence of images.

2 EXPERIMENTAL SETUP

This section describes the flow cell, the image acquisition system and the automated image analysis.

2.1 The flow cell

The required flow channel geometry has to induce a laminar flow field with shear forces strong enough to provoke visible deformation of pulp fibres under laminar flow conditions. The development of the flow cell was carried out in cooperation with the Institute for Fluid Mechanics and Heat Transfer at Graz University of Technology. The flow channel geometry consists of two streams of identical flow rate which are headed against each other in a crossing. The channels are milled into a polycarbonate plate which is screwed together with a plane counterpart to form the 6 [mm] wide and 0.3 [mm] deep channels. The flow cell is shown in Fig. 1a. The channel geometry with dimensions is schematically shown in Fig. 1b.

2.1.1 Suspension transport

To allow for defined flow conditions the flow field has to be stable and undisturbed. Therefore suspension transport needs to be free of pulsations. This is accomplished by using compressed air to pump the suspension through the cell. Two high precision regulating valves are used to supply two pressure resistant glass bottles, equipped with a standpipe and a compressed air connection with the pressure required for the given flow rate. One of the streams is loaded with fibres, one is coloured with black inkjet colour to visualize the distinct line separating the two streams meeting in the crossing (see also Fig. 4b). The flow rate of the coloured stream is monitored using a

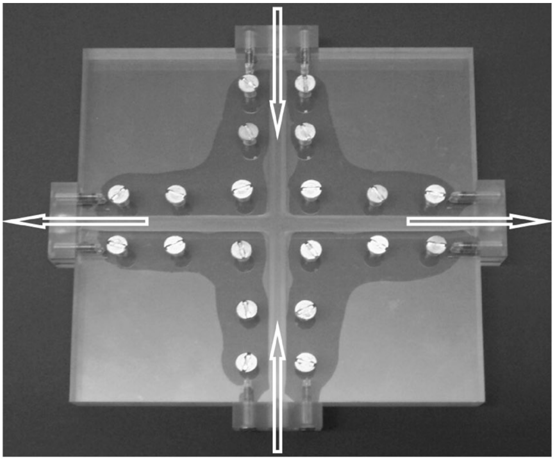

(a)

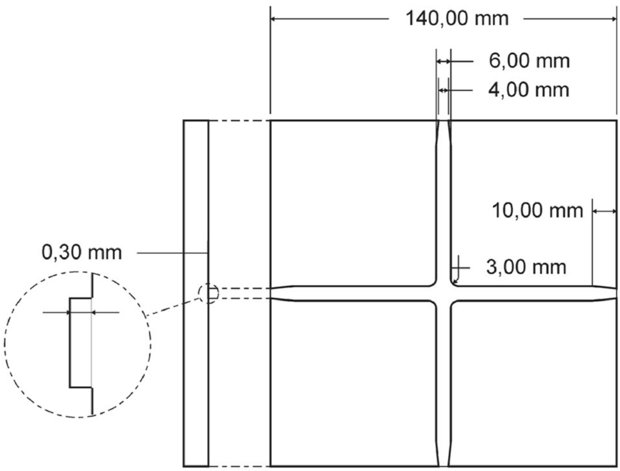

(b)

Figure 1. (a) The flow cell made of polycarbonate. The white arrows indicate the in- and outgoing streams. (b) Flow channel geometry with dimensions.

variable area flow meter to ensure the given flow rate. The line separating the two streams is observed during measurements to ensure the laminarity as well as the equity of the flow rates of the two streams. Fig. 2 shows the suspension flow system schematically.

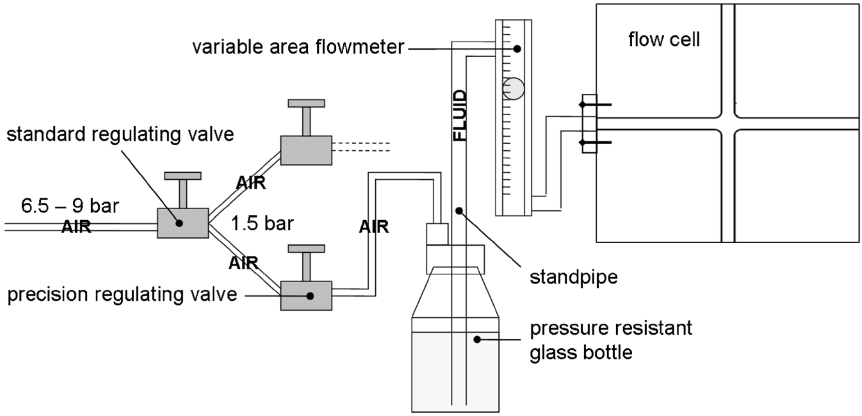

Figure 2. Flow chart for the suspension flow.

2.1.2 Simulation of the flow field

The laminar flow regime was simulated with the commercial CFD software FLUENT® based on the dimensions of the flow cell and the given flow rate of 150 *ml/min* per ingoing channel. The simulation of the flow conditions is performed to determine the velocity distribution as well as the gradients of the velocity in X- and in Y-direction in the centre-symmetry-plane of the the flow geometry (as shown in Fig. 3a). There is no need to determine the whole flow field in Z-direction, as only two-dimensional information concerning the fibres will be accessible in the images. Furthermore, it is assumed that fibres move through the flow geometry oriented along the centre-symmetry-plane. This assumption seems to be valid, as fibres move very stable in the undisturbed channel flow. If a fibre is not oriented in the centre plane it would at some point get contact with the upper or lower wall, or at least with flow conditions close to the wall, which must result in some sort of deflection because of the attached boundary layer. Still, no rotation or any other kind of deflection is observable in the channels with undisturbed flow conditions. As the flow field is symmetrical, not only concerning the centre-symmetry-plane but also concerning the X- and the Y-axes, only one quarter of the flow geometry is simulated (see Fig. 3a).

Concerning the simulation of the fluid flow the forces exerted on the fluid by the suspended fibres are neglected because of the high dilution (≤ 0.01 *g/l*).

The mesh used for simulation has a resolution of 30 μm in the region of high shear forces where the two channels meet each other in the crossing. The

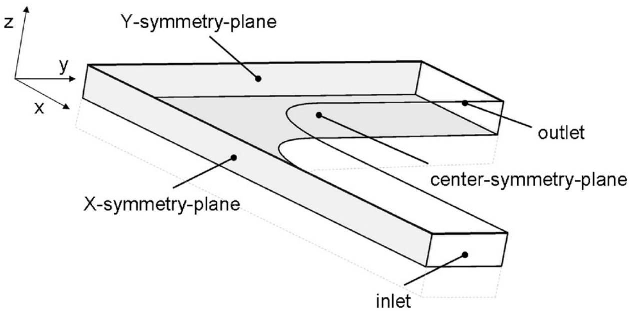

(a)

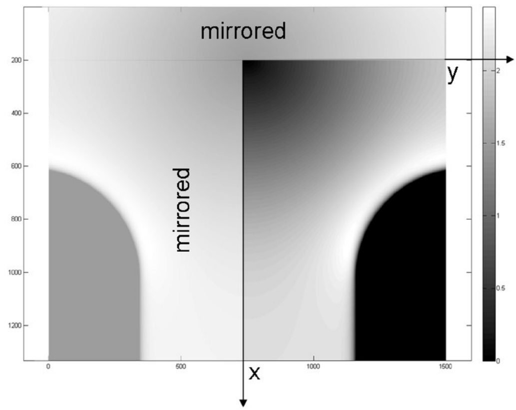

(b)

Figure 3. (a) One quarter of the flow cell with the symmetry planes utilized in the simulation of the flow field. (b) Contour plot of the velocity magnitude, flow field interpolated to image resolution and mirrored through X- and Y-axis.

resolution is decreasing in the ingoing and outgoing channels as their flow field is stable and developed.

Numeric simulation provides values for velocity in X- and Y-direction, the gradients of the velocity components in X- and Y-direction and the velocity magnitude. To be able to link the image information directly with the flow field data without any interpolation necessary during image analysis and evaluation, the flow field data (resolution: 30 μm) is interpolated to the image resolution (7.63 $\mu m/Pixel$) beforehand.

To get the flow field for the whole field of view, the flow data has to be mirrored on the X- and the Y-axis. As only one stream is loaded with fibres and viewed during image acquisition (see also Fig. 1a) only 200 pixels of the flow field are mirrored through he Y-axis, just in case a fibre or part of a fibre trespasses the centreline separating the two streams (which hardly ever happens). The resulting contour plot corresponding to the velocity magnitude with marked mirrored parts is shown in Fig. 3b. As is evident in this image the flow geometry induces a point of zero flow velocity in the centre and high flow velocities close to the curved walls towards the outgoing channels. This high velocity-gradient is the reason for the high shear forces in this region.

2.1.3 Image acquisition system

Images are acquired using a Basler A504k high speed camera. The camera is equipped with a monochrome 1280 × 1024 CMOS progressive scan sensor, provides up to 500 frames per second and allows for an exposure time in the range of 10 *μs* to greater than 33 *msec*.

Images are acquired with a magnification of 3.1 at an optical resolution of 7.63 *μm/Pixel* and a working distance of 75 *mm*. As indicated by the high working distance a macroscope-optic allowing for a high depth of focus is used.

As the fibres move at about 2 *m/s* in the flow cell the lowest possible exposure time of 10 *μs* is required to achieve as distinct images of the fibres as possible. Fibres in the region of higher flow velocities still move up to 2,5 pixels during exposure which is acceptable for further evaluation.

Illumination is done using a high power LED for the highest possible light intensity. Another requirement for the light source is determined by the high working distance. In contrast to diffusive illumination telecentric illumination delivers distinct images of small objects under a high working distance because the light beams beneath the object are blocked and no other light beam tends to interfere with the object. Therefore a telecentric condenser delivering a telecentric light beam with a diameter of 55*mm* is applied.

The frame rate of 500 images per second is sufficient to capture each fibre 3 to 4 times while passing through the region of highest shear forces. The whole measurement system is shown in Fig. 4a, an exemplary image is shown in Fig. 4b.

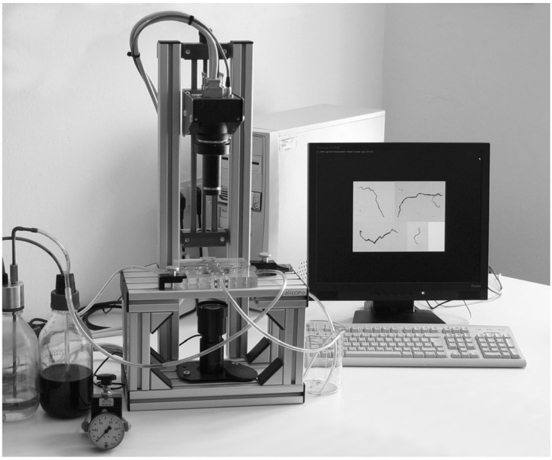

(a)

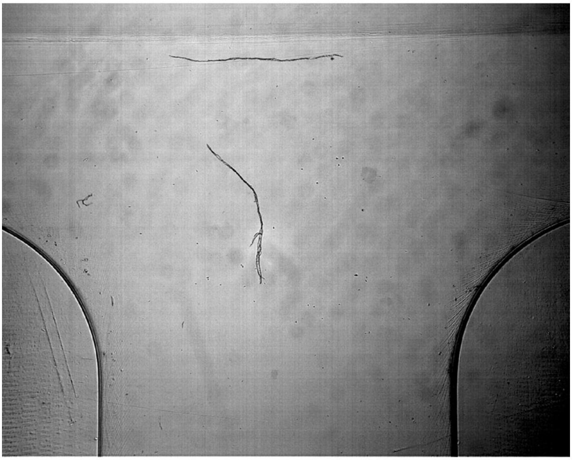

(b)

Figure 4. (a) The measurement system. (b) An exemplary image as it is used for further evaluation.

2.2 Image analysis

For the detection and tracking of individual fibres in the image sequences novel image analysis methods were designed and implemented. Three steps ensure that robust and accurate results are achieved. First, a background correction is applied to the image sequence to highlight the moving fibres in the sequence. Then, individual fibres are detected in every frame and a skeleton representation is calculated for each. Finally, correspondences between the detected fibres in subsequent frames are found in a tracking step. All these steps are done in a fully automated way, thus no user interaction is required.

2.2.1 Background correction

The first step of our framework is the automatic background correction. The goal is to determine pixels in an image, that are significantly different to previous images. In general, background correction methods try to find a model background image, which is then subtracted from the current image highlighting the moving objects. The most simple method for background correction is frame differencing, where changing pixels are solely identified by the difference of the frame at time t and the frame at time $t-1$. Such an approach is not accurate and sensitive to noise. Therefore, we apply a more robust method, which also can be applied in an online manner: the approximated median filter [8]. The approximated median filter computes an approximation of the median value of each pixel over an image sequence by increasing the current estimate by one if the input pixel value is larger than the estimate and by decreasing it by one if smaller:

$$B_{t+1}(m,n) = \begin{cases} B_t(m,n) + 1 & if\ B_t(m,n) < I_t(m,n) \\ B_t(m,n) - 1 & if\ B_t(m,n) > I_t(m,n) \end{cases} \tag{2}$$

where B_t is the estimated background model at frame t and $I_t(m, n)$ is the gray value at the coordinate defined by m and n. In such a way, a binary image is calculated by subtracting the current background model B_t from the current image I_t (step 1 in Fig. 5). The resulting binary image is cleaned of single pixels (step 2 in Fig. 5) and the remaining objects undergo a dilation (step 3 in Fig. 5) followed by an erosion (step 4 in Fig. 5) to close eventual holes within the objects.

Based on this binary image objects that are too close to or in contact with the channel wall are excluded from further evaluation as the velocity gradient in the attached boundary layer is too high to be taken into account for flexibility determination.

2.2.2 Fibre detection and skeletonization

In the second step a skeleton representation of the fibres in the current image is estimated by the following routines: First, the two end points of each fibre

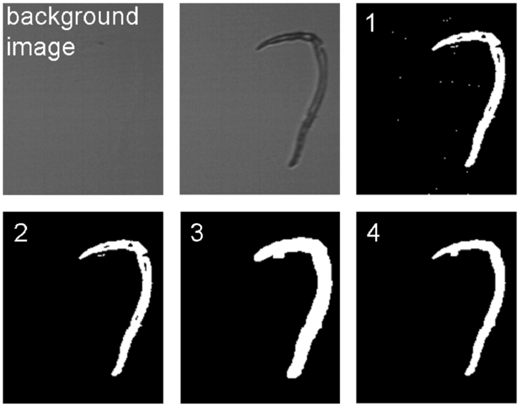

Figure 5. Background-correction and conversion into a binary image; Consecutive steps: 1 . . . only pixels different from the background are considered, 2 . . . cleaning of single pixels, 3 . . . dilation, 4 . . . erosion.

in the image are detected. Then, the detected points are connected to build its skeleton and finally a spline fit provides a smooth skeleton representation.

Since the fibre thickness varies a lot within the images we apply an adapted multi-scale corner detection algorithm to find the end points of the individual fibres as proposed by He *et al.* [9]. Their method finds maximum curvature points in a Curvature Scale Space (CSS) representation. Since coarse and fine features are considered at the same time it is perfectly suited to find the required fibre end points (step 1 in Fig. 6). Then the detected end points of each fibre are connected to get a skeleton representation. Skeletonization

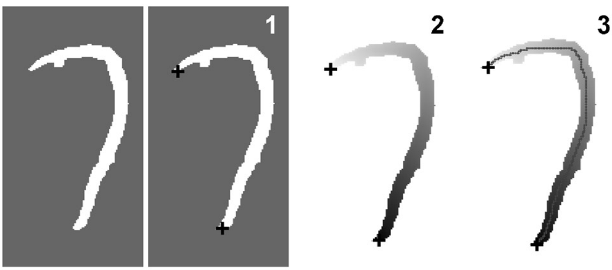

Figure 6. Detection of the fibres centreline; step1 . . . corner detection; step2 . . . calculation of a level-image; step3 . . . determination of the fibre centreline.

aims at reducing the dimensionality of the fibres to a connected free form line while maintaining its topology. We use a combination of state-of-the-art image analysis methods for skeletonization. The main idea is to use a fast marching approach applied on a distance transform map of the fibre segmentations. In general, fast marching [10] allows an efficient formulation for finding the shortest path between two pixels in an image. It only requires a pre-defined cost value for moving from one pixel to a neighbour, which in the simplest case is the gray value difference between them. In our case, we use the inverse of the distance transform of the background corrected binary fibre image as cost, since pixels with a high distance transform value are most likely part of the skeleton. We therefore take one end point of a fibre and apply the fast marching algorithm which estimates the shortest path considering the defined cost to every other pixel in the image (step 2 in Fig. 6). Then, we start at the second end point of the fibre and use a gradient descent method to find the shortest path to the start point, which defines the skeleton of the fibre (step 3 in Fig. 6). The gradient descent is guaranteed to find the shortest path, since the fast marching cost map is convex. In such a way, skeleton representations for all fibres are found in a fully automatic way. Please note, that in contrast to many other available skeltonization methods, it is guaranteed that we find a single connected line between the end points of the fibres, which in addition is always the global optimal solution concerning our pre-defined distance transform energy term.

2.2.3 Tracking of fibres

The output of the second step is a set of skeleton representations of all fibres in the current image. Since we are interested in how fibre skeletons change over the image sequence, we have to link the current set to the set of the previous frame. This tracking step can be done in a very simple manner by comparing the size, length and likely locations of the fibres based on the flow field information. After tracking, a set of skeleton representations for every fibre passing the flow cell is provided.

3 DETERMINATION OF SINGLE FIBRE FLEXIBILITY

The calculation of a fibre's flexibility in terms of the Young's modulus or a bending stiffness requires knowledge of the actual forces acting on the fibre due to the surrounding flow field. The force exerted on a fibre by a fluid flow is defined by the drag coefficient, fibre length, fibre width and the relative velocity fibre – fluid.

Based on the acquired sequence of images only the fibre length can be determined satisfactorily. The fibre width is determinable, but at the given resolution and given the fact that some of the fibres move faster than desirable for distinct images (see 2.1.3), to some extent already afflicted with error. An estimation of the drag coefficient might be possible (see also 4.3.2), but would introduce uncertainties as fibres are very inhomogeneous and the drag coefficient can vary considerably, even along the fibre length. The relative velocity fibre-fluid would have to be determined based on the images of the moving fibre. As the flow conditions can vary considerably between two images (see Fig. 3b), it is hardly possible to determine the velocity of the fibre. Averaging of the rotational and translational part of the fibres movement based on the two images would lead to errors, as it is no steady movement but an accelerated (or decelerated) one.

Considering these shortcomings it was decided that a measurement concept including calculated forces acting on the fibre is not suitable for our method. Too many assumptions introducing measurement uncertainty would have been necessary. A different approach for the determination of single fibre flexibility was chosen, thereby accepting the drawback that no elastic modulus or bending stiffness is retrieved directly.

Based on two fibre images (an example is shown in Fig. 7) against the background of the velocity magnitude, the flexibility of the respective fibre shall be determined. The two fibre images are acquired with a time interval of 2 *ms* (frame rate: 500).

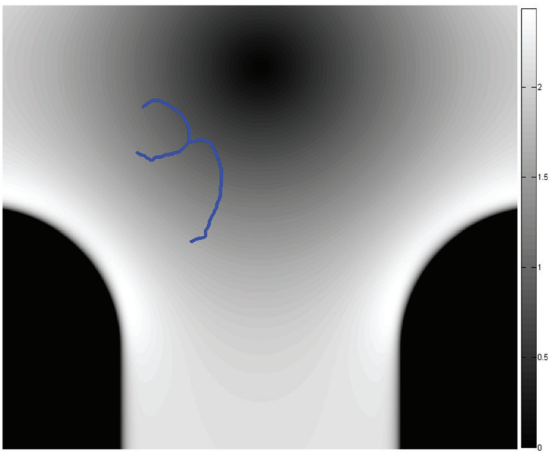

Figure 7. Two consecutive images of the same fibre against the background of the velocity magnitude.

The underlying idea is to compare a specific fibre with an ideally elastic counterpart of identical dimensions and shape. Based on the comparison a flexibility parameter is determined describing how close a fibre's reaction is to that of an ideally elastic one.

Using the simulated flow data it is possible to calculate the streamline a given starting point would follow if it was free of any kind of restraints. Given the first representation of the two fibres shown in Fig. 7 it is possible to calculate the streamline emerging from its centroid (Fig. 8a).

Using the elapsed time span between two consecutive images it is possible to calculate an ideally elastic virtual fibre. Every point along the fibre centre line is allowed to follow its streamline ideally for the given time span. Thereby we get a theoretical ideally elastic fibre which reacted according to the flow field. This ideally elastic fibre is shown in Fig. 8b.

The deformation of this ideally elastic fibre depends on the flow conditions the real fibre is exerted to while passing the sheared region from one image to the other. The higher the load on the fibre during the elapsed time, the stronger is the deformation of the ideally elastic fibre. Thus the deformation of the ideally elastic fibre represents the load on the fibre.

The deformation of the fibre is calculated by comparing the shape of the two fibre representations in question. The comparison is done using euclidean distances. The euclidean distance between two vectors containing parameters describing the fibres appearance is a measure for the similarity of the fibre shapes.

The parameters used for the description of the fibre's shape are the overall fibre curl and the fibre curl of segments of 30 *pixels* along the fibre centre line (about 210 μm of fibre length). By using this segmentwise fiber curl, a fiber showing strong deformation due to a kink acting as some kind of joint will not automatically be considered flexible as only one segment is responsible for the deformation and the euklidian distance remains rather small.

The ideally elastic fibre to some extent varies in length as every point along the fibre centre line moves freely without any restrictions. This is not taken into account for the description of fibre shape (see also 4.3.1), as changes in scale do not affect geometric similarity.

By comparing the fibre we started out with and the same fibre in the consecutive image we get the reaction of the real fibre. Fig. 9a shows the three fibres constituting the basis for the determination of the fibre's flexibility: the first representation of the fibre in the starting image, the calculated ideally elastic fibre and the real fibre as it appears in the consecutive image.

The flexibility parameter assigned to each fibre is defined as the ratio

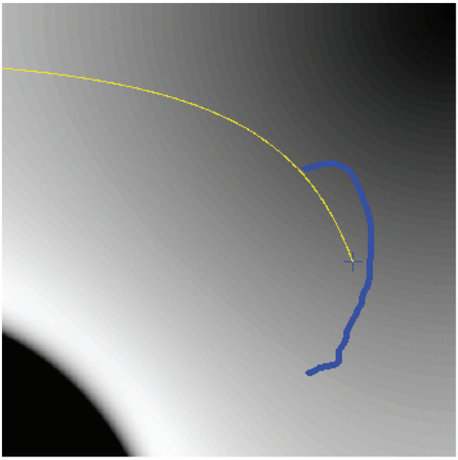

(a)

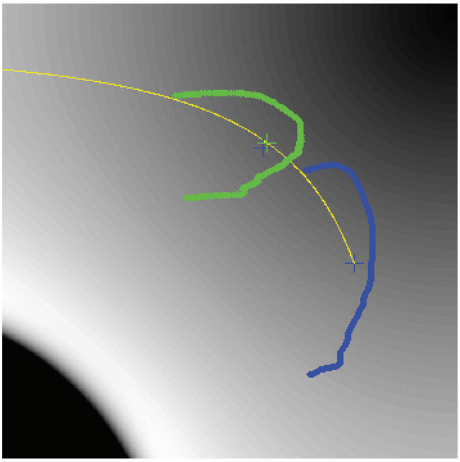

(b)

Figure 8. (a) The streamline emerging from the fibre's centroid. (b) The ideally elastic fibre as it would appear in the consecutive image (light grey).

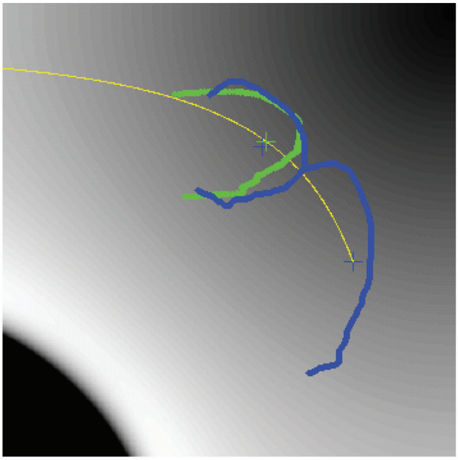

(a)

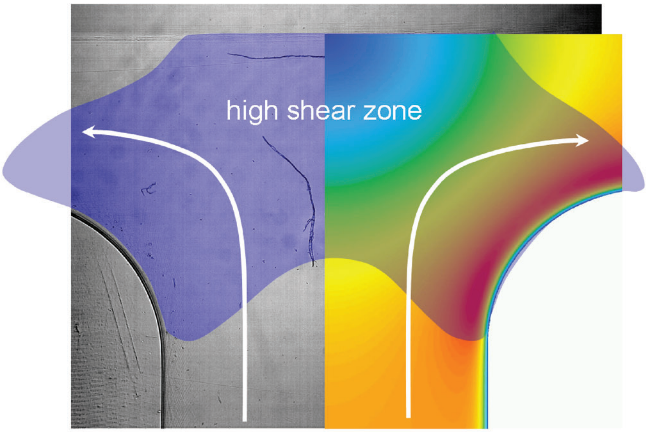

(b)

Figure 9. (a) The real fibre in the two consecutive images (dark grey) and the calculated ideally elastic counterpart (light grey). (b) The region of interest, only fibres within the region of highest shear forces are taken into account for flexibility determination.

between the deformation of the real fibre (Reaction) to the deformation of the ideally elastic fibre (Load):

$$Flexibility = \frac{Reaction}{Load}$$

Reaction . . . Deformation of the fibre from one image to the consecutive one due to the shear forces

Load . . . Deformation of the calculated, ideally elastic fibre due to the shear forces

The flexibility parameter can therefore theoretically vary between zero for a completely rigid fibre (absolutely no reaction) and one for an ideally elastic fibre (meets the deformation of the calculated fibre completely).

Only fibres in the region of high shear forces (exerted to a high load) are considered for flexibility evaluation. A region of interest is defined according to the magnitude of the shear forces and fibres are evaluated only if their centroid lies within this region. The defined region is shown in Fig. 9b with an underlying image as it is acquired by the imaging system and one quarter of the contour plot corresponding to the velocity magnitude.

In addition to this region of interest, only fibres exhibiting a certain deformation of the ideally elastic fibre – a certain load – are accepted for further evaluation. Fibres that pass rather unloaded due to for example good alignment to the stream lines have a high probability for inaccurate flexibility parameters as some sort of ‘reaction’ of the real fibre always arises from image acquisition and image analysis.

4 VALIDATION OF THE METHOD

This section will be used to demonstrate the capabilities and shortcomings of the method. We will show the reproducibility of the measurements. Results based on 4 pulp samples will be cross validated with two other measurement methods and some influences probably affecting the measurement that are not yet taken into account will be discussed. In the end an exemplary result regarding a larger set of industrial samples is presented.

4.1 Reproducibility

Native pulp fibres are very inhomogeneous. To retrieve statistically significant results concerning the average and especially the distribution of fibre morphological parameters a high number of fibres has to be evaluated. Commercial flow cells for example evaluate up to ten thousand and more objects during the assessment of one pulp sample. In our case only objects with a size of greater than 400μm are considered as a fibre. Therefore a smaller sample should already be sufficient. We decided to define an acceptable 95% confidence interval for the average flexibility value and calculate the required number of fibres to assure it.

As described in section 3 flexibility parameter values vary between zero for totally rigid fibres and one for ideally flexible ones. The maximum size of the 95% confidence interval for the average flexibility value was predefined as 0.005.

To assess the required number of fibres a population of 4000 fibres of a softwood kraft pulp sample as well as 4000 fibres of a regenerate fibre sample were measured. The regenerate fibre was a staple fibre with a dtex value of 0.9 and a varying length of 1.5 to 7 mm. The staple fibre was used because of the homogeneous composition compared to native pulp fibres. A comparison between pulp fibres and staple fibres can therefore give an impression concerning the origin of the variability in the measurement results as one part of it will arise from the measurement principle and the other from the inhomogeneity of the pulp fibres.

Sample sets of fibres were chosen from the population. The number of fibres in the sets varied stepwise between 500 and 1500. For each amount of fibres 400 sample sets were chosen and the mean value, as well as the 95% confidence interval for this mean value was calculated. These confidence intervals decreased for rising numbers of fibres in the sample sets. Fig. 10 shows the size of the confidence intervals over the number of fibres per

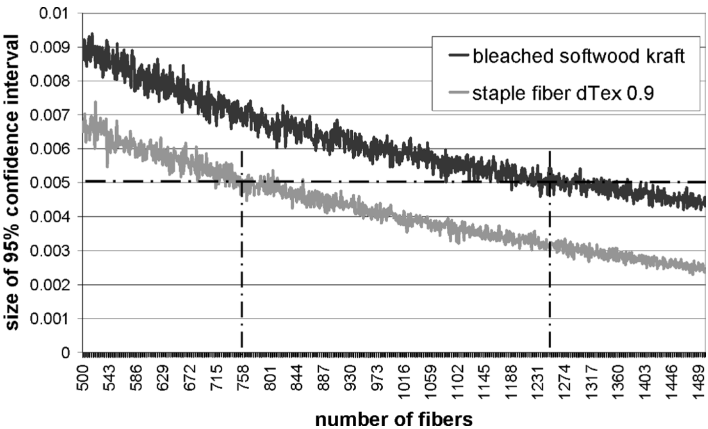

Figure 10. The size of the confidence intervals for the mean flexibility parameter over the number of fibres per sample set.

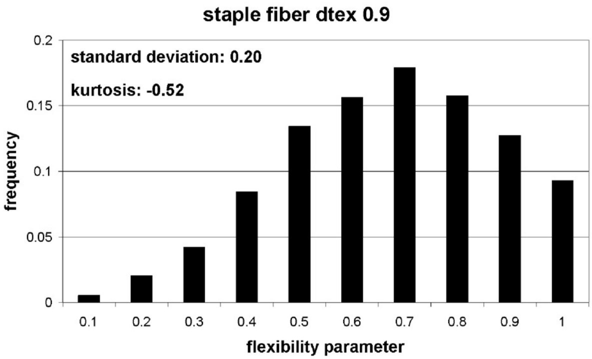

(a)

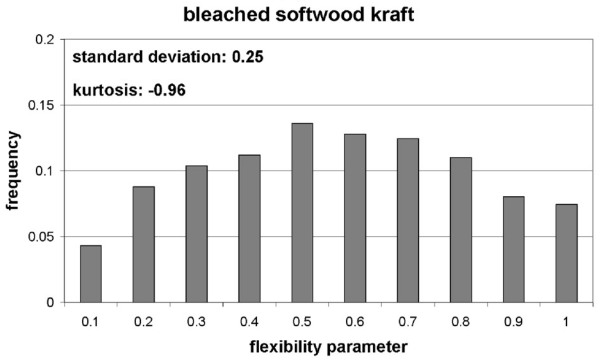

(b)

Figure 11. The distributions of fibre flexibility for the staple fibre and the softwood kraft pulp sample.

sample set. The lines represent the predefined size and thereby the required number of fibres per measurement. 750 measured staple fibres are necessary for the predefined statistical significance compared to 1250 fibres for the native pulp sample.

The standard deviation and the kurtosis are chosen as parameters to describe the distribution of the flexibility parameter. Thereby the staple fibre serves as a reference. Fig. 11a+b show the distributions of the flexibility parameter for these two samples. Standard deviation as well as kurtosis are given in the diagrams.

For the evaluation of at least 1.000 fibres, we have to take 4.000 images.

Given a wet pulp sample, sampling and image acquisition is done within about 15 minutes. Image analysis as well as further evaluation is implemented in Matlab which is easy to use but has a poor runtime performance. The automated evaluation of 4.000 images lasts about 8 hours which could be reduced by several magnitudes if the routines were implemented in C+.

4.2 Cross validation

Two other methods were used to validate our results based on four different pulp samples. The measurement methods were:

- MorFi fibre morphology analyzer; offers an average flexibility index that is based on the average fibre curl at different shear rates [1]
- The method developed by Tam Doo and Kerekes [4] that was already discussed in 1. The method delivers the bending stiffness [Nm^2] respectively the flexibility [$1/Nm^2$] for each evaluated fibre.

50 fibres per sample were evaluated with the TamDoo method for these validation measurements.

The pulp samples used for validation in ascending order concerning their expected flexibility were:

- high yield softwood kraft pulp (kappa value of 42)
- bleached softwood kraft pulp
- the same bleached softwood kraft pulp after 10.000 revolutions in a PFI-mill
- staple fibre; dtex 0.9, varying length of 1.5 to 7 mm (see also 4.1)

The results of the three measurement methods are shown in Fig. 12. The staple fibre could not be measured with the MorFi device as the fibres are very flexible and plugged the flow cell due to spinning. Only nine of the fifty measured staple fibres delivered a result with the TamDoo method. The high flexibility also led to measurement errors.

The confidence intervals for the results retrieved with the TamDoo method are rather wide due to the low number of evaluated fibres and a rather wide range of flexibility values retrieved per measured fibre (e.g. flexibility values for the BSK sample ranged from 0.05 to 2.69) [$1/Nm^2$]. Nevertheless, the relation between the samples shows the expected result and the flexibility parameter retrieved with the newly developed method can thereby be related to actual flexibility values (see Fig. 12 in the upper left).

Confidence intervals for the MorFi measurements were not accessible. The results do not show the expected ascending order, the PFI-mill treated sample should exhibit higher flexibility than the untreated one.

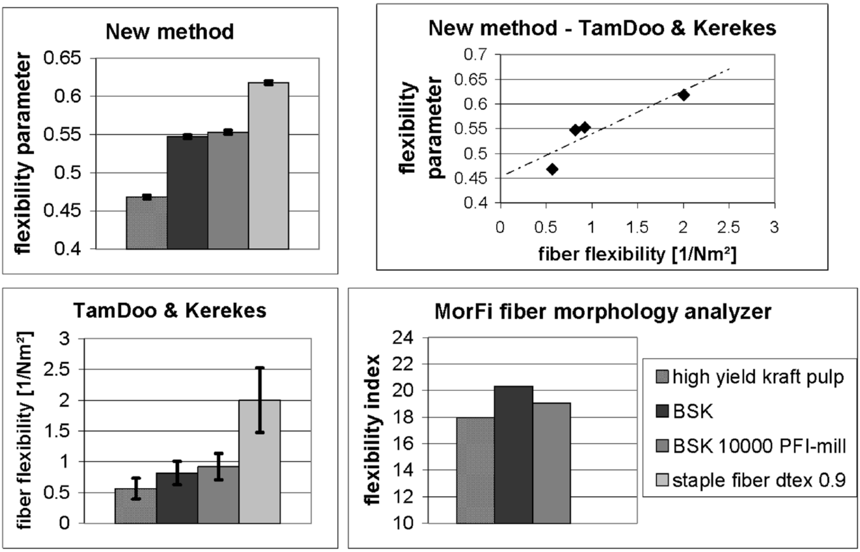

Figure 12. Average flexibility parameter of the four samples for validation for the three measurement methods.

4.3 Influences affecting the measurement

As is evident in section 4.1 the distributions of the evaluated flexibility parameter are rather wide spread, with considerable amounts of fibres in the classes of almost totally rigid or ideally elastic fibres. The wide spread distribution is expected to some extent, as pulp fibres are very inhomogeneous. But still, as the fibres are allowed to move freely in the flowing suspension, uncertainties concerning their movement have to be accepted.

Besides these uncontrollable uncertainties some measurable influencing parameters are not yet taken into account in the evaluation of fibre flexibility.

4.3.1 Fibre length

The obtained results indicate the influence of fibre length. Longer fibres are by trend assigned higher flexibility values than shorter ones.

Fibres are not only exposed to bending forces but also to buckling or elongation. These forces are represented by the variation in length of the ideally elastic fibre discussed in section 3. Taking these length changes into account diminishes or even eliminates the influence of fibre length on the obtained results. On the other hand, tests have shown that taking the fibre length into account for the comparison of shape constituting the basis for the obtained flexibility parameter leads to less accurate results.

4.3.2 Drag coefficient

Another influencing parameter is the drag coefficient of the fibres. The higher the drag coefficient, the higher are the fluid forces acting on the fibre and higher deformations will be observed. As described in the following, a measure indicating the drag coefficient can be determined based on the acquired images.

The fibre does not follow the fluid flow ideally, because of a its rigidity and its inertia. Using the frame rate and flow field data it is possible to calculate where a certain particle in the flow regime should emerge in the following frame. If this is done for the centre of gravity of a fibre a deviation between calculated and real centre of gravity may arise. Evaluating the deviation of about 7000 fibres we get the image shown in Fig. 13a. Depending if the fibre is captured in an accelerated or decelerated part of the flow field it is slower or faster than the fluid flow due to inertia effects. The amount of deviation must depend to a high extent on the drag coefficient of the fibre, a higher drag coefficient allows the fibre to follow the fluid flow closer and therefore leads to smaller deviation.

As an example we evaluated a softwood kraft pulp sample treated in the PFI-mill for 1000, 7000 and 15000 revolutions. Different values of average deviation according to the increased fibrillation and therefore changed drag coefficients were evident (see Fig. 13b).

Yet, no improvement of measurement results could be achieved by taking this information that is available for each evaluated fibre into account.

4.4 Exemplary result

A sample set consisting of 14 commercial softwood kraft pulps of different suppliers bleached to a brightness of 85 to 90 was evaluated. All samples were once dried and unbeaten. The average flexibility values for these samples ranged between 0.46 and 0.56.

No linear correlation was evident to laboratory sheet parameters like bulk or porosity which are widely recognized as influenced by fibre flexibility. But if the average fibre flexibility together with length weighted fibre length was used to describe the bulk of the sheet, a clear correlation could be found as is shown in Fig. 14.

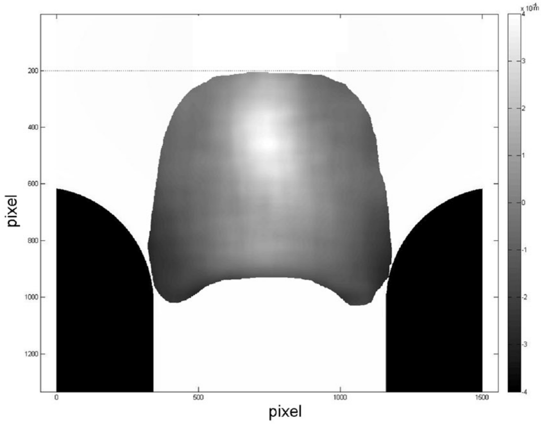

(a)

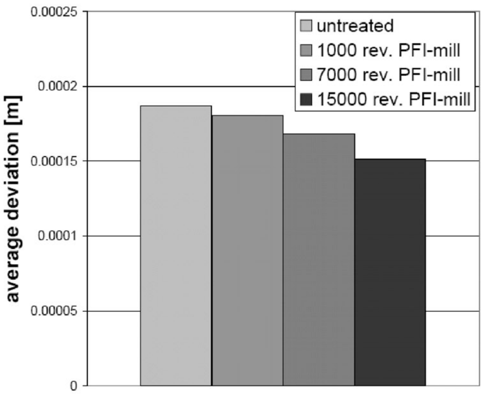

(b)

Figure 13. (a) Contour plot of the deviation of the centre of gravity based on 7000 fibres (flow channel geometry in the background). Bright areas: fibres faster than fluid. Dark areas: fibres slower than fluid. (b) Average deviation of 4 pulp samples after increasing PFI treatment showing decreasing deviation of the centre of gravity due to fibrillation.

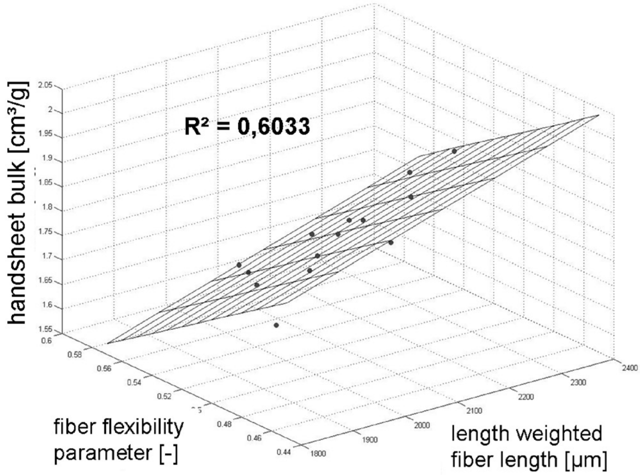

Figure 14. Correlation map for 14 softwood kraft pulp samples.

5 CONCLUSIONS

A new method for single fibre flexibility measurement was presented in this paper. The method is based on the fibre's reactions to defined shear forces in a special channel geometry. No flexibility or bending stiffness in terms of an elasticity modulus but a dimensionless flexibility parameter is obtained. As the fibres are suspended in water, the method has potential on line applicability in a flow cell based fibre morphology analyzer. fibre flexibility parameters already delivered by some commercially available flow cells are average parameters for the whole pulp sample, whereas our device delivers single fibre based values and can therefore provide fibre flexibility distributions. Comparisons with other measurement methods and first applications on industrial pulp samples show that the method delivers meaningful results.

The distributions are rather wide spread also indicating some uncertainties in the measurment. Although information on the homogeneity of the fibre sample concerning fibre flexibility is already accessible based on these distributions, further improvements are necessary to reduce the uncertainty and thereby enhance the significance of these distributions.

ACKNOWLEDGEMENTS

The authors gratefully acknowledge financial support of the Austrian Research Promotion Agency Ltd. (FFG) and of Andritz AG, Poels AG, Sappi Gratkorn, SCA Graphic Laakirchen, Smurfit Nettingsdorfer Papierfabrik and the Delfort Group.

REFERENCES

1. STFI. Method and Apparatus for Measuring Fibre Flexibility. International Publication Number: WO 92/05423:International Publication Date: 02. April 1992, International Patent Classification: G01N 15/02.
2. Trepanier R.J. Kuhn D.C.S., Huang Z. and Patchka H. Dynamic Wet Fiber Flexibility Analyzer. *TAPPI Procedings/Process and Product Quality Conference and Trade Fair*, pages 67–710, 1997.
3. Samuelson L.G. Measurement of the Stiffness of Fibers. *Svensk Paperstidning*, **66**(15):541–546, 1963.
4. Tam Doo P.A. and Kerekes R.J. A Method to Measure Wet Fiber Flexibility. *Tappi Journal*, **64**(3): 113–116, 1981.
5. Olson J.A. Kuhn D.C.S., Lu X. and Robertson A.G. A Dynamic Wet Fibre Flexibility Device. *Journal of Pulp and Paper Science*, **21**(10):J337–J342, 1995.
6. Forgacs O.L. Arlov A.P. and Mason S.G. Particle Motion in Sheared Suspension. *Svensk Paperstidning*, **61**(3):61–67, 1958.
7. Meindersma E. Robertson A.A. and Mason S.G. The Measurement of Fiber Flexibility. *Pulp and Paper Magazine of Canada*, **62**(1):T3–T10, 1961.
8. Nigel J. B. McFarlane and C. Paddy Schofield. Segmentation and tracking of piglets. *Machine Vision and Applications*, **8**(3):187–193, 1995.
9. X.C. He and N.H.C. Yung. Curvature scale space corner detector with adaptive threshold and dynamic region of support. In *Proceedings of International Conference on Pattern Recognition (ICPR)*, volume **2**, 2004.
10. J. Sethian. *Level set methods*. Cambridge University Press, 1996.

Transcription of Discussion

SINGLE FIBRE FLEXIBILITY MEASUREMENT IN A FLOW CELL BASED DEVICE

Rene Eckhart,[1] *Michael Donoser*[2] and *Wolfgang Bauer*[1]

[1]Institut for Paper, Pulp and Fibre Technology,
Graz University of Technology
[2]Institute for Computer Graphics and Vision, Graz University of Technology

Ilya Vadeiko FPInnovations

In one of your last slides, you showed that there is a relationship between the flexibility, in the way you define it, and the fibre length (figure 14 in the paper in the proceedings, ed.). I was wondering if you had tried to look into some kind of normalized flexibility; normalized to the fibre lengths?

Rene Eckhart

Weighted fibre length and measured fibre flexibility of the 14 evaluated samples showed a good correlation to the handsheet bulk. As far as I remember there was no direct correlation between fibre flexibility and weighted length for these samples.

But your question is a good one and I mentioned this matter in the paper. Within one pulp sample the fibre flexibility the answer is "Yes" and "No", dependent on fibre length.

The calculated ideally elastic fibre that is used to define the load on a respective fibre allows changes in length, as it can be elongated or shortened due to the fluid flow. If I use these length changes in the description of fibre shape for the calculation of fibre deformation, there is no dependency of the resulting fibre flexibility on fibre length. On the other hand, the accuracy of the results decreases, which means it gets harder to distinguish between samples known to have differing flexibility. Therefore it's hard to decide whether to use these length changes in the description or not.

Discussion

Ilya Vadeiko

To me it seemed logical that, depending on how you define the vector of parameters describing the fibre shape, you may have different definitions of your flexibility, and I was wondering if there is an optimized way to define the structure of parameters that would also refer to the fibre lengths in some way.

Rene Eckhart

That is what I meant when I said there might be some opportunity to improve the distributions by improving the set of parameters. At the moment, I do not use fibre length. I accept that my fibre flexibility parameter is to some extent dependent on fibre length, but the results are more accurate that way, at least for the time being.

Ilya Vadeiko

So, a final comment on this. When you show the results for a real pulp and you showed the fairly wide distribution of fibre flexibility, could this also be related to the fact that you had a distribution of fibre lengths?

Rene Eckhart

Yes, it is linked to the flexibility.

James Olson University of British Columbia

First a comment and then a question. I was very interested in your work because I worked with David Kuhn and his Masters student, Lu, on a similar project a long time ago. My comment is that it was not just mentioned once, it was published in the Journal of Pulp and Paper Science, but in 1995.

Rene Eckhart

I thought the concept was slightly different in the paper presented in 1995. Wasn't the fibre assumed to be in contact with the capillary walls and thereby treated as a supported beam?

James Olson

No, it was still injected.

Rene Eckhart

Okay.

James Olson

And the second thing: a problem we always had was that we could never tell whether or not, if we had a curled fibre, whether it would straighten out by bending or whether it would rotate and just appear straighter, even though it did not actually straighten. I just want to know how you got around that.

Rene Eckhart

I think that is not a problem in my system. If a curled fibre would rotate, and thereby seem to be straightened, it would at the same time undergo a change in the visible fibre length. In our system, image analysis as well as tracking of the fibres is automated. The tracking algorithms depend to a great extent on fibre length. If the length changes between two consecutive images, the fibre will no longer be tracked and will not be available for flexibility determination. I think this covers this problem.

Elias Retulainen VTT

The flexibility of the fibre varies along the length of the fibre, so I wonder how your number reacts when you have, let us say, a stiff fibre with one very flexible hinge in the middle of the fibre?

Rene Eckhart

In my parameter set for the description of fibre shape I use the curl of segments along the fibre. If the fibre deforms due to some kind of joint, only one of these segments would be affected; the rest of the parameter set would remain rather similar. Therefore it's different if the deformation is related to a joint or if the fibre bends over the whole length. This would be represented in the resulting flexibility parameter.

Jula Salmela VTT

Very interesting presentation, and a nice way to measure fibre flexibility. Can you comment on, or have you tried to measure, the effect of fibres on the flow field? I mean for homogeneous fibres you get a very wide spread of the flexibility index. So I guess one reason is that the fibres affect the flow field, and the flow field is not ideal in the flow cell. Have you tried to measure how big is the effect using PIV or something?

Rene Eckhart

No, I did not go into this. I am sure the fibres affect the flow field, but I have not dealt with these problems yet.

Jula Salmela

Okay. So, what is your opinion? How big is the effect of a non-ideal flow field due to the fibres, and is this the main reason for wide flexibility index distribution?

Rene Eckhart

Currently my opinion is that these wide distributions are due to the fact that the fibre's interaction with the surrounding fluid varies due to differences, for example, in the surface of the fibre. Today we have already heard about the "envelope" of fluid surrounding a suspended fibre and I am quite sure this is also influenced by the surface of the fibre, for example, due to fibrillation. Therefore the movement of the fibre, the load the fluid exerts on the fibre and, as a result, the reaction of the fibre do vary considerably – not only due to differences in flexibility, but also due to the differing interaction with the surrounding fluid. But, as the resolution of my images is not sufficient, I cannot address these differences in fibre surface or take them into account in the measurement concept.

Tetsu Uesaka FPInnovations

This is probably a comment rather than a question. The fibre flexibility has been measured by many people with various difficulties and obviously the instrumentation part is getting more and more sophisticated like yours. My question is that every time this fibre flexibility is measured, there is a question, a very persistent question: is it necessary to measure it?

Rene Eckhart

I hope so.

Tetsu Uesaka

What people do, and also what we did so far, is to try to correlate with bulk and other properties such as cell wall thicknesses, etc. There are already expected kinds of parameters that we can chase in terms of process control. So we always wonder, is it really necessary to measure this parameter? So I am just asking your opinion after yours efforts.

Rene Eckhart

Well, my job at our institute is fibre characterization and I somehow have to do something. I am not sure if it is necessary, but that is what I do.

In my opinion it is desirable to be able to measure as many single-fibre properties as possible in an on-line manner, for example in the approach flow. Thereby a model describing the resulting paper parameters based on these single-fibre parameters will be more and more reliable, and maybe can be used to adjust the stock preparation immediately. Other parameters already covered by commercially available flow cells, like coarseness and fibre wall thickness, may be somewhat correlated to fibre flexibility, but in my own experience the correlation to coarseness is not always that clear and, although I have not investigated it yet, I think it will be similar with fibre wall thickness. Therefore, as I have already mentioned, I think that the more parameters that are measureable in such a flow cell based device the better.

Gary Baum PaperFuture Technologies.

Very interesting paper. I have a question of clarification that may be related to some of the earlier questions. You define load as the deformation of the ideal elastic fibre due to shear forces and I just want to make sure you mean local shear forces at that point of the fibre. Are you using the same shear force for all points along the fibre, or are you using the local shear at each point along the fibre length?

Rene Eckhart

No, every point along a fibre's centre line is linked to the corresponding flow conditions. The mesh used for simulation of the flow field had a resolution of 30 microns and I interpolated it down to 15 microns. Thereby every point along the fibre is treated in the way it should be.

Discussion

Gary Baum

I understood. Thank you.

Torbjörn Wahlström Stora Enso

You have investigated 13 kraft pulp samples. In mechanical pulping, we want to treat thick-walled long fibres and I guess they are less flexible than the thin walled fibres. One usage here would be to identify the thick walled long fibres before and after treatment and see how we succeed in treating just those fibres compared to others. Have you made measurements on mechanical fibres?

Rene Eckhart

When we started with the development of the method, one of the first tasks was to provoke shear forces strong enough to deform fibres. We also used a TMP sample for these tests and some, but not all, of the fibres could be deformed by the shear forces. There may be some restrictions to application in the field of mechanical pulps, but basically it should work. Still, the experiments I have done so far were all performed on chemical pulp fibres.